

# 000 001 002 003 004 005 006 007 008 009 010 011 012 013 014 015 016 017 018 019 020 021 022 023 024 025 026 027 028 029 030 031 032 033 034 035 036 037 038 039 040 041 042 043 044 045 046 047 048 049 050 051 052 053 WAVE: LEARNING UNIFIED & VERSATILE AUDIO- VISUAL EMBEDDINGS WITH MULTIMODAL LLM

Anonymous authors

Paper under double-blind review

## ABSTRACT

While embeddings from multimodal large language models (LLMs) excel as general-purpose representations, their application to dynamic modalities like audio and video remains underexplored. We introduce WAVE (**u**nified & **v**ersatile **a**udio-**v**isual **e**mbeddings), the first LLM-based embedding that creates a unified representation space for text, audio, and video modalities. WAVE employs a novel hierarchical feature fusion strategy and a joint multi-modal, multi-task training approach to enable two key capabilities: any-to-any cross-modal retrieval and the generation of prompt-aware embeddings tailored to user instructions. Experimentally, WAVE sets a new state-of-the-art on the MMEB-v2 video benchmark and achieves superior results in audio and video-to-audio retrieval. Its prompt-aware nature also yields remarkable performance in multimodal question answering, significantly outperforming existing embedding models. Ablation studies validate our joint training strategy, demonstrating improved performance across all modalities. With a newly introduced benchmark for versatile audio-visual learning, WAVE opens up broad possibilities for cross-modal, any-to-any applications. Our code, checkpoints, and data will be released.

## 1 INTRODUCTION

Multimodal embeddings, which transform diverse data types such as text, images, video, and audio into a shared representation space, are central to cross-modal search, classification, and recommendation. The prevailing approach employs separate encoders per modality that are aligned in a common space (Radford et al., 2021; Jia et al., 2021; Zhai et al., 2023; Ma et al., 2022; Miech et al., 2020; Xu et al., 2021; Elizalde et al., 2023; Mei et al., 2024; Guzhov et al., 2022; Su et al., 2024; McKee et al., 2023; Chen et al., 2024b). Recently, the success of large language models (LLMs) has catalysed a more integrated paradigm: using a single multimodal LLM (MLLM) to produce embeddings for all modalities jointly. This shift is enabled by increasingly capable MLLMs that can process and reason over images (Liu et al., 2024b;a; Li et al., 2023; Chen et al., 2023), audio (Tang et al., 2024; Gong et al., 2024; 2023; Chu et al., 2024), and video (Li et al., 2025a; Zhang et al., 2025c; Liu et al., 2025b; Zhu et al., 2025; Bai et al., 2025; Li et al., 2025b; Zhang et al., 2025a; Xu et al., 2025; Tang et al., 2025). Consequently, the field is rapidly moving toward using these models to produce potent, versatile multimodal embeddings (Jiang et al., 2025; Meng et al., 2025; Yu et al., 2025a; Zhang et al., 2024; Jiang et al., 2024; Gu et al., 2025; Lin et al., 2025; Liu et al., 2025a).

A unified embedding paradigm built upon MLLMs fully leverages their strengths in semantic understanding and representation. By processing all modalities within a single model, this approach naturally improves cross-modal interoperability and semantic alignment, which benefits downstream tasks such as retrieval. Such a model can also ingest multiple modalities concurrently to form holistic representations—for example, a coherent embedding from paired audio and video streams. Furthermore, by inheriting the instruction-following capabilities of MLLMs, the resulting embeddings can be prompt-aware, conditioning on user instructions to encode task-relevant semantics. Despite these advantages, most MLLM-based embedding efforts have concentrated on vision, particularly static images, while underexploring audio and synchronised audio-visual streams. Consequently, the promise of a truly universal audio-visual embedding space remains largely unrealised.

To address these limitations, we introduce WAVE, a **u**nified & **v**ersatile **a**udio-**v**isual **e**mbedding MLLM. To the best of our knowledge, WAVE is the first model to produce unified embeddings

for text, audio, silent video, and synchronised audio–visual inputs. Built on Qwen2.5-Omni (Xu et al., 2025), WAVE projects heterogeneous inputs into a shared semantic space, enabling seamless cross-modal interaction. Experiments confirm that WAVE produces powerful embeddings, achieving state-of-the-art (SOTA) performance on the MMEB-v2 video track (Meng et al., 2025) and excelling at tasks like any-to-any retrieval (e.g., text-to-video, video-to-audio). Moreover, it can generate prompt-aware embeddings for downstream applications like multimodal question answering (QA). Crucially, WAVE maintains or even surpasses the performance of the base Qwen2.5-Omni on multimodal understanding benchmarks, which is notable since most embedding models show a significant decline in these capabilities compared to their foundational MLLMs.

Our main contributions can be summarised as follows:

- **Versatile audio–visual embedding MLLM:** We introduce WAVE, the first audio–visual embedding MLLM capable of producing unified, general-purpose representations for text, audio, silent video, and synchronised audio–visual inputs. By projecting heterogeneous modalities into a single semantic space, WAVE excels at challenging any-to-any retrieval and achieves SOTA performance on the MMEB-v2 video track.
- **Instruction-following for prompt-aware embeddings:** Leveraging the instruction-following ability of its MLLM backbone, WAVE generates prompt-aware multimodal embeddings. Unlike conventional models that yield task-agnostic representations, WAVE can condition embeddings on a user’s task-specific prompt, which is reflected in its strong results on embedding-based multimodal QA.
- **Effective architecture:** We propose a hierarchical feature-fusion strategy that aggregates representations from multiple MLLM layers, yielding stable gains on tasks such as multimodal retrieval. In addition, a dual-encoder design for audio captures complementary cues (e.g., speech and environmental sounds), further enhancing the expressiveness of the learned embeddings.

## 2 BACKGROUND

### 2.1 MULTIMODAL REPRESENTATION LEARNING

Multimodal representation learning seeks to construct a shared embedding space in which text, image, audio, and video can be compared and composed. A major milestone is CLIP (Radford et al., 2021), which uses contrastive learning with dual encoders to align images and text at scale. Building on this paradigm, ALIGN (Jia et al., 2021) shows that training on even larger, noisier corpora, exceeding a billion image–text pairs, yields strong gains on retrieval and classification. SigLIP (Zhai et al., 2023) further simplifies and scales training by replacing the standard InfoNCE objective with a sigmoid loss, removing the need for in-batch negatives and improving efficiency.

This contrastive recipe naturally extends to video. X-CLIP (Ma et al., 2022) adapts the dual-encoder design to video–text retrieval with explicit temporal modelling. To better exploit large but noisy web videos, Miech et al. (2020) enhance contrastive learning with noise-contrastive estimation, enabling learning from loosely aligned narration. VideoCLIP (Xu et al., 2021) strengthens discrimination by mining hard negatives via nearest-neighbour retrieval during training.

In audio–language learning, CLAP (Elizalde et al., 2023) aligns audio and text in a joint space, enabling zero-shot audio classification and cross-modal retrieval. To address the scarcity of high-quality paired data, Mei et al. (2024) introduce the WavCaps corpus and build state-of-the-art audio–language retrieval models with HTSAT (Chen et al., 2022a) and BERT (Devlin et al., 2019).

As audio and vision are naturally synchronised and complementary, learning unified audio–visual representations is an important next step. AudioCLIP (Guzhov et al., 2022) generalises CLIP to a trimodal setting (audio, image, text), enabling richer cross-modal transfer. Su et al. (2024) propose a unified framework for audio–visual representation and generation, and subsequent work explores emerging applications such as video-to-music retrieval (McKee et al., 2023; Chen et al., 2024b).

### 2.2 LLM-BASED EMBEDDING MODELS

Pretrained on vast corpora, LLMs exhibit strong semantic understanding and broad world knowledge, motivating their use as text-embedding generators. Two common strategies adapt decoder-

only LLMs into embedding models: *last-token pooling*, which takes the hidden state of the end-of-sentence (EOS) token as the sentence embedding, and *mean pooling*, which averages token-level hidden states. Using last-token pooling, Wang et al. (2024) first synthesize training data with proprietary LLMs and then fine-tune target models with a standard contrastive objective, yielding competitive text embeddings without complex pipelines. NV-Embed (Lee et al., 2025a) removes the causal attention mask and introduces a latent attention layer to improve mean pooling. More recently, Gemini Embedding (Lee et al., 2025b), Qwen3 Embedding (Zhang et al., 2025b), and QZhou-Embedding (Yu et al., 2025b) have set new marks on comprehensive benchmarks such as MTEB (Muennighoff et al., 2022) through large-scale training.

In the multimodal setting, researchers extend MLLMs to carve out a unified semantic space across modalities, aiming to produce robust, general-purpose embeddings with a single model. VLM2Vec (Jiang et al., 2025) is an early effort that trains a visual LLM across diverse multimodal embedding tasks; VLM2Vec-V2 (Meng et al., 2025) broadens coverage to video and documents. Zhang et al. (2024) focus on multimodal retrieval, building an MLLM-based universal retriever for images and text, while E5-V (Jiang et al., 2024) shows that training on text pairs alone can still improve image–text retrieval. MM-Embed (Lin et al., 2025) adopts an image-LLM bi-encoder with modality-aware hard-negative mining to mitigate modality bias. Gu et al. (2025) combine textual discriminative distillation with multimodal contrastive learning to construct an image embedding LLM. LamRA (Liu et al., 2025a) offers a general framework that equips visual LLMs with strong retrieval and re-ranking, and CAFE (Yu et al., 2025a) unifies visual representation learning and generation via a contrastive-autoregressive fine-tuning scheme, enabling a single model to excel at both retrieval and image generation.

### 3 METHODS

#### 3.1 MODEL ARCHITECTURE

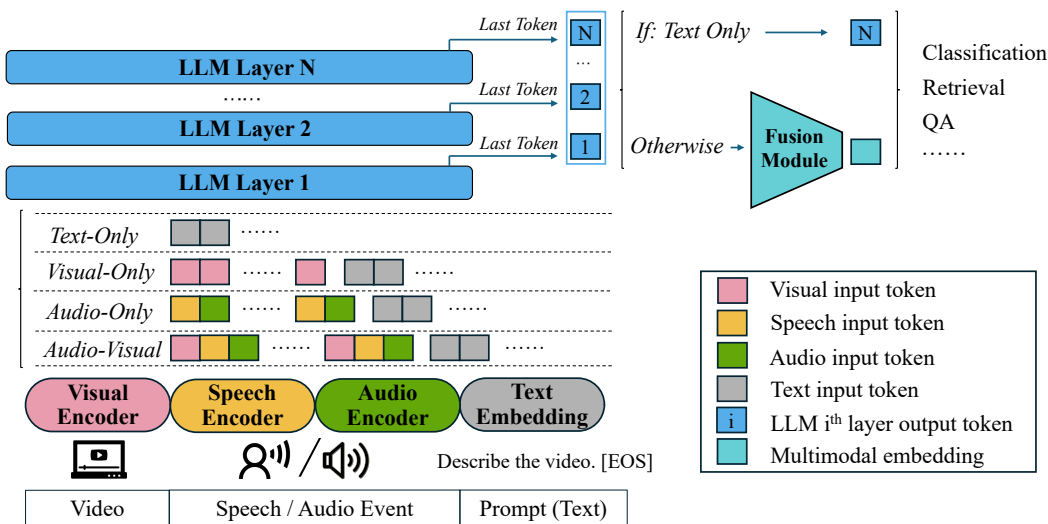


Figure 1: Inputs can be text-only, vision-only, audio-only, or audio–visual. For text-only cases, the final embeddings are obtained via last-token pooling over the LLM’s last hidden states. For multimodal inputs, the last output tokens from all LLM layers are concatenated and passed to a feature-fusion module to produce a unified multimodal embedding. Note that text prompts are always provided to instruct the LLM for multimodal inputs.

The overall architecture of WAVE is shown in Fig. 1. The model can accept text, video frames, audio signals, or synchronised audio-visual data as input and generate multimodal embeddings for downstream tasks, such as classification, retrieval, and QA.

To handle this modality diversity, WAVE employs distinct encoders for non-text inputs. A pre-trained visual encoder extracts features from video frames, converting them into visual tokens for

162 the LLM. For audio, we utilise a dual-encoder architecture to comprehensively capture the input  
 163 signal. A speech encoder and a separate audio encoder generate speech-related and audio event-  
 164 related tokens, respectively. Text inputs are tokenised using the LLM’s original embedding layer.  
 165 Crucially, all non-text inputs are accompanied by a text prompt, which serves as an instruction to  
 166 the LLM.

167 **To structure the multimodal input tokens for the LLM, we employ specific interleaving strategies.**  
 168 **For audio-only input, the speech-related and audio event-related tokens, which are equal in number**  
 169 **due to identical encoder frequencies, are interleaved on a one-to-one basis to form a unified auditory**  
 170 **token sequence. For synchronised audio-visual input, both the visual and auditory token sequences**  
 171 **are partitioned into several segments corresponding to the number of sampled frames. These seg-**  
 172 **ments are then interleaved to create the audio-visual token sequence. Finally, the text tokens of the**  
 173 **prompt are appended to the end to form the input token sequence for the LLM.**

174 There are four possible input configurations: text-only, visual-only, audio-only, and audio-visual.  
 175 Among them, audio and video are both multimodal temporal signals. To enhance the LLM’s ability  
 176 to capture spatiotemporal structure, we adopt the time-aligned multimodal rotary position Embed-  
 177 **ding (TMRoPE) introduced in Qwen2.5-Omni (Xu et al., 2025). Because the speech and audio en-**  
 178 **coders are synchronised to produce outputs at the same frequency, their tokens are naturally aligned**  
 179 **in time. Tokens corresponding to the same frame, therefore, share the same TMRoPE, ensuring**  
 180 **precise temporal alignment.**

181 After TMRoPE is applied, the multimodal token sequence is fed into the LLM. Inspired by the use of  
 182 the hidden state of the final “EOS” token by last-token pooling, we aggregate the last output tokens  
 183 from multiple LLM layers to construct embeddings for non-text modalities. This design captures  
 184 both low-level perceptual cues and high-level semantic abstractions. A lightweight fusion mod-  
 185 **ule—implemented as a two-layer multi-layer perceptron (MLP) with GELU activation (Hendrycks**  
 186 **& Gimpel, 2016) is then used to refine and compress the embeddings. For the text-only scenario,**  
 187 **we retain the standard last-token pooling approach, which prior studies have shown to be highly**  
 188 **effective.**

### 189 3.2 TRAINING STRATEGY

190 Similar to previous work, we adopt contrastive learning as the primary training paradigm to align  
 191 representations from different modalities into a unified embedding space. The semantic similarity  
 192 between any two embeddings is quantified using the cosine similarity metric.

193 Our training regimen is composed of two distinct but complementary tasks: multimodal retrieval  
 194 and QA. The retrieval task requires the model to extract general multimodal embeddings with a  
 195 general prompt like “Describe the video”, while the QA task requires the model to extract prompt-  
 196 aware embeddings that well interpret the given question. During training, each sample provides a  
 197 source-target pair of inputs, denoted as  $(s, t)$ , which are processed by the model to produce their  
 198 respective embeddings,  $e_s$  and  $e_t$ . The training is performed on mini-batches of size  $N$ , and we  
 199 build a task-aware data sampler that ensures samples in the mini-batch belong to the same task.

200 **Retrieval Task:** For the retrieval task,  $s$  and  $t$  belong to different modality types, which can be  
 201 any of the supported formats: text-only, audio-only, visual-only, or audio-visual. This allows for  
 202 arbitrary any-to-any cross-modal training. We employ an in-batch negative sampling strategy, where  
 203 for a given positive pair, all other non-corresponding pairs within the mini-batch are treated as  
 204 negative samples. To ensure a robust alignment, we compute a symmetric InfoNCE loss.

205 Specifically, for the  $i$ th sample in the mini-batch, when its source embedding  $e_{s_i}$  serves as the query  
 206 and its target embedding  $e_{t_i}$  is the positive key, the loss  $L_{s_i}$  is formulated as a cross-entropy loss  
 207 over the batch:

$$208 \mathcal{L}_{s_i} = -\log \frac{\exp(\text{sim}(e_{s_i}, e_{t_i})/\tau)}{\sum_{j=1}^N \exp(\text{sim}(e_{s_i}, e_{t_j})/\tau)}, \quad (1)$$

209 where  $\text{sim}(\cdot, \cdot)$  denotes the cosine similarity,  $\tau$  is the temperature parameter, and the summation in  
 210 the denominator is over all target embeddings  $e_{t_j}$  in the mini-batch. For the retrieval task, the source  
 211  $s$  and target  $t$  are interchangeable. Therefore, the symmetrical scenario is also considered, where  $e_{t_i}$   
 212 serves as the query and  $e_{s_i}$  is the positive key. The symmetrical loss  $\mathcal{L}_{t_i}$  is:

216  
217  
218  
219

$$\mathcal{L}_{t_i} = -\log \frac{\exp(\text{sim}(e_{t_i}, e_{s_i})/\tau)}{\sum_{j=1}^N \exp(\text{sim}(e_{t_i}, e_{s_j})/\tau)}. \quad (2)$$

220 The final retrieval loss for the entire mini-batch is the average of these individual losses over all  
221 samples and both directions, ensuring a bidirectional alignment:222  
223  
224  
225

$$\mathcal{L}_{\text{Retrieval}} = \frac{1}{2N} \sum_{i=1}^N (\mathcal{L}_{s_i} + \mathcal{L}_{t_i}). \quad (3)$$

226 **Question Answering Task** : For the QA task, the source  $s_i$  for the  $i$  th sample in the mini-batch  
227 is a multimodal signal accompanied by a textual prompt that poses a question. The corresponding  $t_i$   
228 is a text-only input representing the correct answer. To train the model for this discriminative task,  
229 we augment each sample with a set of  $n$  incorrect or “distractor” answers, denoted as  $\{t'_{i,k}\}_{k=1}^n$ .  
230 The model then extracts embeddings for the correct answer,  $e_{t_i}$ , and for each incorrect answer,  
231  $\{e'_{t_{i,k}}\}_{k=1}^n$ . The objective is to maximise the probability of selecting the correct answer from the  
232 candidate pool. The QA loss for the  $i$  th sample,  $\mathcal{L}_{\text{QA}_i}$ , is thus formulated as a cross-entropy loss:233  
234  
235

$$\mathcal{L}_{\text{QA}_i} = -\log \frac{\exp(\text{sim}(e_{s_i}, e_{t_i})/\tau)}{\exp(\text{sim}(e_{s_i}, e_{t_i})/\tau) + \sum_{k=1}^n \exp(\text{sim}(e_{s_i}, e'_{t_{i,k}})/\tau)}. \quad (4)$$

236 This objective function effectively trains the model to produce a multimodal query embedding  $e_{s_i}$   
237 that is most similar to the embedding of the correct textual answer  $e_{t_i}$ , while being distant from the  
238 embeddings of incorrect answers. The total QA loss for the batch is the average of individual losses:239  
240  
241  
242

$$\mathcal{L}_{\text{QA}} = \frac{1}{N} \sum_{i=1}^N \mathcal{L}_{\text{QA}_i}. \quad (5)$$

243  
244

## 4 EXPERIMENTAL SETTINGS

245  
246

### 4.1 MODEL SPECIFICATIONS

247  
248  
249  
250  
251  
252  
253  
254  
255  
256  
257

WAVE is built on the 7 billion (B) parameter version of Qwen2.5-Omni (Xu et al., 2025). Specifically, the LLM backbone, the visual encoder, and the speech encoder are all initialised from the pre-trained weights of Qwen2.5-Omni, which allows WAVE to inherit the powerful multimodal perception and reasoning capabilities of the foundation model. For the dedicated audio encoder, we adopt BEATs encoder (Chen et al., 2022b) and further append a trainable aligner to align its output with the LLM’s input space. The aligner consists of a two-layer MLP projector with a GELU activation function. To ensure efficient fine-tuning, we employ the low-rank adaptation (LoRA) (Hu et al., 2022) technique on the LLM backbone. The LoRA modules are configured with a rank of 128 and a scaling factor of 2.0. A dropout rate of 0.05 is applied to the LoRA modules during training to mitigate overfitting. To generate the ultimate multimodal embeddings, a two-layer MLP with a GELU activation function serves as the fusion module to fuse features from different layers of the LLM. The temperature  $\tau$  of the model is set to 0.01.

258  
259  
260  
261  
262  
263

As for the model input, videos, in general, are sampled at 2 frames per second, with a maximum of 128 frames sampled. For videos longer than 64 seconds, 128 frames are uniformly sampled to conserve memory resources. [The maximum resolution for each frame is 176400 pixels](#). For audio input, the waveform signals are resampled to 16,000 Hz. [Other preprocessing settings are identical to those of Qwen2.5-Omni](#).

264  
265

### 4.2 TRAINING SPECIFICATIONS

266  
267  
268  
269

Before the large-scale contrastive learning, we perform a dedicated pre-training phase for the BEATs aligner. This stage aligns the BEATs encoder with the backbone LLM so that the LLM can interpret BEATs features. Only the aligner’s parameters are updated while all other components remain frozen. Given an audio clip and a simple text prompt (for example, ‘Please describe the audio’), the model is trained to generate a descriptive audio caption. Training uses audio from WavCaps (Mei

et al., 2024), AudioCaps (Kim et al., 2019), and Clotho (Drossos et al., 2020); clips longer than 180 seconds are discarded to avoid memory issues. We train for three epochs on 128 H20 GPUs.

Next, we proceed with the primary training stage as detailed in Section 3.2. Table 2 provides a comprehensive overview of the multimodal tasks, data sources, the modalities of each sample pair  $(s, t)$ , and the number of data samples used in our training. Notably, we re-annotate the 1 million (M) videos of the Panda-70M dataset (Chen et al., 2024a) using InternVL-2.5-8B (Chen et al., 2024c). Besides, in some datasets, a video may correspond to multiple text captions. To enhance the diversity of text captions, we construct samples that share the same video but differ in text captions for these datasets. The final WAVE model is trained on 192 H20 GPUs for one epoch, and the total training time is approximately 36 hours. We set the learning rate to  $2 \times 10^{-5}$ , and configure a per-device batch size of 1, resulting in a total batch size of 192. The data sampler is designed to ensure that samples in each training mini-batch are consistent in task types and data sources. The visual aligner and the LoRA module are trainable in this stage, while other modules will stay frozen. For ablation experiments, the training settings are similar except that we only use 128 H20 GPUs for training.

Table 1: An overview of training tasks and data. Four tasks are trained for our models: video-text retrieval, video-QA, video-audio retrieval and audio-text retrieval.

Task	Data Source	Modalities of $(s, t)$	# Samples
Video-Text Retrieval	Panda-70M (Chen et al., 2024a)	(visual, text)	1.0 M
	MSVD (Chen & Dolan, 2011)	(visual, text)	24 K
	DiDeMo (Anne Hendricks et al., 2017)	(visual, text)	8 K
	ActivityNet Captions (Krishna et al., 2017)	(visual, text)	10 K
	MSR-VTT (Xu et al., 2016)	(audio-visual, text)	180 K
	VATEX (Wang et al., 2019)	(audio-visual, text)	260 K
	YouCook2 (Zhou et al., 2018)	(audio-visual, text)	10 K
Video-QA	Shot2Story (Han et al., 2023)	(audio-visual, text)	530 K
	LLaVA-Video-178k (Zhang et al., 2025c)	(visual, text)	100 K
Video-Audio Retrieval	AudioSet (Gemmeke et al., 2017)	(audio, visual)	1.7 M
	VGGSound (Chen et al., 2020)	(audio, visual)	182 K
Audio-Text Retrieval	AudioCaps (Kim et al., 2019)	(audio, text)	49 K
	AudioSet-SL (Hershey et al., 2021)	(audio, text)	108 K
	Clotho (Drossos et al., 2020)	(audio, text)	19 K
<b>Total</b>	-	-	4.9 M

### 4.3 EVALUATION SPECIFICATIONS

To thoroughly assess the performance of WAVE, we have collected and organised a comprehensive suite of evaluation tasks and benchmarks. This collection is designed to systematically measure the quality of the embeddings for each modality and to validate the model’s cross-modal alignment capabilities.

Details of the evaluation data and metrics are shown in Table 2. All evaluation tasks are formulated as “query-to-target” retrieval. For video-centric tasks, we adopt the video subset from MMEB-v2 (Meng et al., 2025) as our foundation, and we also augment the evaluations on the recent benchmark LoVR (Cai et al., 2025). In the audio domain, our evaluation encompasses both retrieval and QA tasks as well. Beyond these text-centric scenarios, more challenging tasks such as video-to-audio retrieval and video-to-music retrieval are evaluated, which test the model’s ability to map visual semantics to auditory concepts directly within its unified embedding space. [More details of the inference procedure for each evaluation task are shown in Appendix B.](#)

## 5 EXPERIMENTAL RESULTS

### 5.1 OVERALL RESULTS

The results of our model are shown in Table 3 and Table 4. WAVE demonstrates its capabilities to generate versatile multimodal embeddings, achieving strong performance across a range of video,

324  
325 Table 2: Details of the evaluation benchmarks. We formulate all tasks as “query-to-target” retrieval,  
326  
327

Data Source	Task	Subset	(Query, Target) Modalities	Metrics
MMEB-v2-Video (Meng et al., 2025)	Classification	CLS	(visual, text)	Acc%
	Video QA	QA	(visual, text)	Acc%
	Retrieval	RET	(text, visual/audio-visual)	R@1
	Moment retrieval	MRET	(text, visual)	R@1
LoVR (Cai et al., 2025)	Retrieval	text-to-clip theme-to-clip	(text, visual)	R@1 R@25
AudioCaps (Kim et al., 2019)	Retrieval	test	(text, audio)	R@1
Clotho (Drossos et al., 2020)	Retrieval	test	(text, audio)	R@1
VGGSound (Chen et al., 2020)	Retrieval	test	(visual, audio)	R@1
MusicCaps (Agostinelli et al., 2023)	Retrieval	test	(visual, audio)	R@1
MMAU (Sakshi et al., 2025)	Audio QA	test-mini	(audio, text)	Acc%
MMAR (Ma et al., 2025)	Audio QA	test	(audio, text)	Acc%

341 audio, and audio-visual scenarios. In the video domain, WAVE comprehensively outperforms ex-  
342 isting open-source models across all sub-tasks on the video track of MMEB-v2, which systemati-  
343 cally evaluates various video understanding capabilities. Notably, the overall performance of our  
344 model even surpasses that of the industrial-grade model, Seed-1.6-Embedding<sup>1</sup>. Furthermore, our  
345 model also exhibits strong performance on LoVR, not only on caption-based text-to-clip retrieval but  
346 also on concept-based theme-to-clip retrieval, leading existing open-source multimodal embedding  
347 LLMs.

348 Table 3: Results of video embedding benchmarks. Models are evaluated on the video track of  
349 MMEB-v2 and LoVR.

Model	MMEB-v2-Video					LoVR	
	Overall	CLS	QA	RET	MRET	text-to-clip	theme-to-clip
LamRA 7B (Liu et al., 2025a)	35.0	39.3	42.6	24.3	32.8	62.9	60.2
GME 7B (Zhang et al., 2024)	38.4	37.4	50.4	28.4	37.0	51.2	43.9
CAFé 7B (Yu et al., 2025a)	42.4	35.8	58.7	34.4	39.5	-	-
Seed-1.6-Embedding	55.3	55.0	60.9	51.3	<b>53.5</b>	-	-
WAVE 7B	<b>59.9</b>	<b>57.8</b>	<b>72.5</b>	<b>54.7</b>	50.8	<b>62.9</b>	<b>66.0</b>

358 Table 4: Results of audio and audio-visual embedding benchmarks. Different tasks are evaluated,  
359 including audio retrieval (A-RET), audio-visual retrieval (AV-RET) and audio QA (A-QA).  
360

Method	A-RET		AV-RET		A-QA	
	AudioCaps	Clotho	VGGSound	MusicCaps	MMAU	MMAR
Reference Model	(Mei et al., 2024)		encoder-only retrieval model (ours)		Qwen2.5-Omni 7B	
Reference Value	42.2	21.5	10.3	8.6	71.5	56.7
WAVE 7B	<b>44.2</b>	<b>25.6</b>	<b>25.0</b>	<b>20.4</b>	<b>76.6</b>	<b>68.1</b>

361 In the audio domain, on the widely used AudioCaps and Clotho datasets, WAVE achieves superior  
362 audio retrieval performance compared to previous models that rely on separate-encoder architec-  
363 tures. Moreover, as a unified multimodal embedding model, WAVE is also capable of video-to-audio  
364 retrieval, a more challenging task that directly bypasses the text modality. For a fair comparison, we  
365 train an encoder-only retrieval model (columns 4 and 5 in Table 4) using the same video-to-audio  
366 retrieval data, where video embeddings are extracted by WAVE’s visual encoder and audio embed-  
367 dings are extracted by WAVE’s speech and audio encoders. The results in Table 4 show that WAVE  
368 considerably outperforms the encoder-only retrieval model on audio-visual retrieval, not only on the  
369 in-domain VGGSound test set but also on the out-of-domain video-to-music MusicCaps data.  
370

371 [More evaluation results are shown in Appendix C.](#)  
372

373 <sup>1</sup><https://seed.bytedance.com/en/blog/built-on-seed1-6-flash-seed-1-6-embedding-launched>

378  
379

## 5.2 ANALYSIS OF PROMPT-AWARE EMBEDDINGS

380  
381  
382  
383  
384

Beyond retrieval, WAVE leverages its LLM backbone’s reasoning to produce prompt-aware embeddings conditioned on textual instructions (see Appendix D for a case study). The ability to follow instructions is crucial for embedding MLLMs in QA tasks, which can be shown by the following question example from Video-MME (Fu et al., 2025): *Which of the following features/items is not discussed in the video in relation to the tomb? A. Inkstone. B. Niche. C. Jade. D. Sacrificial table.*

385  
386  
387  
388  
389

Models that cannot understand the input question may probably produce an embedding that represents the main content of the video, which will lead to incorrect predictions. We list the detailed QA results in Table 5. To investigate the extent to which text prompts contribute to WAVE’s ability to generate embeddings, we also instructed WAVE with a common prompt (“Please describe the video”) when testing, instead of separate questions.

390

391  
392  
393  
394

Table 5: Results of different models on MMEB-v2 video QA data, including Video-MME (Fu et al., 2025), MVBench (Li et al., 2024), NExT-QA (Xiao et al., 2021), EgoSchema (Mangalam et al., 2023), and ActivityNetQA (Yu et al., 2019). In the case of “w/ separate questions”, each question is used as a different prompt.

395  
396  
397  
398  
399  
400  
401  
402  
403  
404

Model	MMEB-v2-Video QA					
	Average	Video-MME	MVBench	NExT-QA	EgoSchema	ActivityNetQA
LamRA 7B	42.6	34.1	37.2	43.7	44.8	53.2
GME 7B	50.4	39.2	46.6	53.6	46.8	65.6
CAFe 7B	58.7	46.0	48.9	62.4	60.0	76.0
Seed-1.6-Embedding	60.9	54.0	53.3	66.2	52.2	78.6
WAVE 7B, w/ a common prompt	51.8	39.3	44.7	53.5	61.4	60.2
WAVE 7B, w/ separate questions	<b>72.5</b>	<b>63.4</b>	<b>69.6</b>	<b>82.6</b>	<b>66.2</b>	<b>80.9</b>

405  
406  
407  
408  
409  
410

Compared with existing embedding MLLMs, WAVE outperforms strong baselines when testing with separate questions, averaging about 12% higher than Seed-1.6-Embedding. However, using general prompts to extract embeddings leads to a drastic performance degradation across all QA datasets. This stark contrast not only highlights the strong instruction-following capability of WAVE, but also suggests the critical limitation of a single, static representation for complex tasks like multimodal QA.

411  
412  
413  
414

On audio-reasoning benchmarks, WAVE further surpasses its base, Qwen2.5-Omni model, as Table 4 shows. This is notable given that WAVE was trained only to generate question-conditioned embeddings for video QA. This cross-modal transfer underscores robust generalisation and supports the hypothesis that WAVE learns a unified, modality-agnostic embedding space.

415

416

## 5.3 BENEFIT OF JOINT MULTI-MODAL, MULTI-TASK TRAINING

417  
418  
419  
420  
421  
422  
423

A core hypothesis behind our unified model is that joint training across diverse modalities and tasks fosters a more robust and powerful universal embedding space. We posit that learning from audio, video, and text data simultaneously enables positive knowledge transfer, where insights from one modality can enhance the understanding of another. To verify this, we conducted an ablation study comparing our fully-trained WAVE model against specialist models trained on modality-specific subsets of the data.

424  
425  
426  
427  
428  
429

Specifically, using the data described in Table 1, we train models under the following three task settings: training video-text retrieval and video-QA, training audio-text retrieval, and training video-audio retrieval. Each model is trained on only one fixed pair of modalities, without mixing data from other modalities. Then we test the three separately trained models on video, audio, and audio-visual benchmarks, respectively. The results are shown in Table 6, denoted as “Separate”. The final WAVE model jointly trained across all modalities is also reported for comparison, denoted as “Joint”.

430  
431

As shown in Table 6, the model trained jointly across modalities outperforms separately trained specialist models on seven of eight tasks, indicating positive cross-modal knowledge transfer. Exposure to richer, more diverse signals encourages learning generalised, modality-agnostic seman-

432  
 433 Table 6: Comparison of model performance under separate vs. joint training schemes. The model  
 434 jointly trained on all modalities and tasks consistently outperforms specialist models trained on  
 435 separate modality-task pairs.

Training	MMEB-v2-Video					A-RET		AV-RET	
	Overall	CLS	QA	RET	MRET	AudioCaps	Clotho	VGGSound	MusicCaps
Separate	58.2	57.5	71.6	<b>56.1</b>	47.6	42.5	24.0	24.9	20.1
Joint	<b>59.0</b>	<b>57.8</b>	<b>72.5</b>	54.7	<b>50.8</b>	<b>44.2</b>	<b>25.6</b>	<b>25.0</b>	<b>20.4</b>

441  
 442  
 443 tic representations rather than modality-specific features, underscoring the promise of a model for  
 444 general-purpose embedding extraction.

#### 445 5.4 ANALYSIS OF FEATURE FUSION

446  
 447 When using an LLM for embedding extraction, a common choice is last-token pooling, which takes  
 448 the EOS token’s hidden state from the final layer as the sequence representation. However, as Gou  
 449 et al. (2025) observe, different LLM layers specialise in distinct functions for video understanding,  
 450 implying complementary information is distributed across depth. Accordingly, we aggregate signals  
 451 from all layers to form the final embedding, preserving both low-level perceptual cues and high-level  
 452 semantic reasoning. Concretely, we collect the last-token states from every layer, concatenate them,  
 453 and feed them to a lightweight fusion module to produce the output embedding.

454  
 455 To efficiently assess embedding-extraction strategies while conserving compute, we conduct an ex-  
 456 panded ablation primarily on pure-visual (no-audio) video retrieval, with an additional check in the  
 457 audio-visual setting. Evaluations use the MMEB-v2 video-retrieval split. Beyond the two main  
 458 strategies, **1**) standard last-token pooling from the final LLM layer and **2**) our all-layer last-token  
 459 MLP fusion, we also test **3**) the last-token output from the first layer, **4**) the last-token from a middle  
 460 layer (Layer 15), and **5**) a learnable weighted sum (Peters et al., 2018) of last-token features across  
 461 all layers. The LLM has twenty-eight layers in total. Results are shown in Table 7.

462  
 463  
 464 Table 7: Results of embedding extraction methods on the MMEB-v2 video retrieval data, including  
 465 MSR-VTT, VATEX, MSVD, DiDeMo, and YouCook2. Note that videos in MSR-VTT, VATEX, and  
 466 YouCook2 are paired with audio. “V” and “A+V” refer to visual-only and audio-visual, respectively.

Method	Modality	MMEB-v2-Video RET					
		Average	MSR-VTT	VATEX	MSVD	DiDeMo	YouCook2
Last token pooling (first layer)		38.8	44.8	37.3	60.9	39.0	12.0
Last token pooling (middle layer)		45.0	48.9	41.4	67.5	47.3	17.8
Last token pooling (last layer)	V	49.6	52.1	46.2	<b>69.7</b>	53.0	27.2
All-layer last token weighted sum		48.3	49.4	45.6	69.4	50.6	26.3
All-layer last token MLP fusion		<b>50.5</b>	<b>53.6</b>	<b>47.5</b>	68.7	<b>55.4</b>	<b>27.3</b>
Last token pooling (last layer)	A+V	54.7	58.2	56.3	69.3	54.8	34.9
All-layer last token MLP fusion		<b>56.1</b>	<b>58.5</b>	<b>58.4</b>	<b>69.3</b>	<b>57.4</b>	<b>36.8</b>

477  
 478 As shown in Table 7, using only first-layer or middle-layer features yields a marked drop versus the  
 479 final-layer representation, consistent with a hierarchical abstraction in which the top layer carries  
 480 the most semantically relevant information for retrieval. Early-layer cues are still useful, however:  
 481 fusing last-token features from all layers with a small MLP consistently surpasses the strong last-  
 482 layer baseline. By contrast, a direct weighted sum across layers underperforms, suggesting that  
 483 cross-layer interactions for video tasks are complex and non-linear, and thus benefit from learned  
 484 transformations. The pattern holds in the audio-visual setting, our all-layer MLP fusion again out-  
 485 performs last-layer pooling, and Table 7 further shows that audio substantially boosts video retrieval,  
 reinforcing the value of a unified, general-purpose multi-modal embedding model.

486 **6 CONCLUSION**  
 487

488 We present WAVE, to our knowledge, the first unified, versatile audio–visual embedding MLLM that  
 489 maps text, audio, silent video, and synchronised audio–visual inputs into a single semantic space. A  
 490 dual audio-encoder design combined with hierarchical all-layer feature fusion yields robust, com-  
 491 prehensive multimodal representations. Joint multi-modal, multi-task training enables WAVE to  
 492 achieve strong results (e.g., on the MMEB-v2 video track) and to generate prompt-aware embed-  
 493 dings that translate into competitive multimodal QA performance. Ablations confirm the benefits  
 494 of unification—showing positive cross-modal transfer and the value of learned cross-layer fusion.  
 495 WAVE establishes a new, powerful baseline for universal audio-visual representation learning and  
 496 can serve as a springboard for cross-modal, any-to-any applications.  
 497

498 **7 REPRODUCIBILITY STATEMENT**  
 499

500 We provide detailed descriptions of the model architecture, training pipelines, training data and  
 501 hyperparameters in Sections 3.1, 3.2, 4.1, and 4.2. All datasets, code, and model checkpoints will  
 502 be released. These provide enough reproducibility for our work.  
 503

504 **REFERENCES**  
 505

506 Andrea Agostinelli, Timo I Denk, Zalán Borsos, Jesse Engel, Mauro Verzetti, Antoine Caillon,  
 507 Qingqing Huang, Aren Jansen, Adam Roberts, Marco Tagliasacchi, et al. MusicLM: Generating  
 508 music from text. *arXiv preprint arXiv:2301.11325*, 2023.

509 Lisa Anne Hendricks, Oliver Wang, Eli Shechtman, Josef Sivic, Trevor Darrell, and Bryan Russell.  
 510 Localizing Moments in Video with Natural Language. In *Proc. ICCV*, Venice, 2017.

511 Shuai Bai, Keqin Chen, Xuejing Liu, Jialin Wang, Wenbin Ge, Sibo Song, Kai Dang, Peng Wang,  
 512 Shijie Wang, Jun Tang, et al. Qwen2.5-VL technical report. *arXiv preprint arXiv:2502.13923*,  
 513 2025.

514 Qifeng Cai, Hao Liang, Hejun Dong, Meiyi Qiang, Ruichuan An, Zhaoyang Han, Zhengzhou Zhu,  
 515 Bin Cui, and Wentao Zhang. LoVR: A benchmark for long video retrieval in multimodal contexts.  
 516 *arXiv preprint arXiv:2505.13928*, 2025.

517 David Chen and William B Dolan. Collecting highly parallel data for paraphrase evaluation. In  
 518 *Proc. ACL-HLT*, Portland, 2011.

519 Honglie Chen, Weidi Xie, Andrea Vedaldi, and Andrew Zisserman. VGGSound: A large-scale  
 520 audio-visual dataset. In *Proc. ICASSP*, Barcelona, 2020.

521 Ke Chen, Xingjian Du, Bilei Zhu, Zejun Ma, Taylor Berg-Kirkpatrick, and Shlomo Dubnov. HTS-  
 522 AT: A Hierarchical Token-semantic Audio Transformer for Sound Classification and Detection.  
 523 In *Proc. ICASSP*, Singapore, 2022a.

524 Sanyuan Chen, Yu Wu, Chengyi Wang, Shujie Liu, Daniel Tompkins, Zhuo Chen, and Furu Wei.  
 525 BEATs: Audio pre-training with acoustic tokenizers. *arXiv preprint arXiv:2212.09058*, 2022b.

526 Tsai-Shien Chen, Aliaksandr Siarohin, Willi Menapace, Ekaterina Deyneka, Hsiang-wei Chao,  
 527 Byung Eun Jeon, Yuwei Fang, Hsin-Ying Lee, Jian Ren, Ming-Hsuan Yang, et al. Panda-70M:  
 528 Captioning 70M videos with multiple cross-modality teachers. In *Proc. CVPR*, Seattle, 2024a.

529 Zeyu Chen, Pengfei Zhang, Kai Ye, Wei Dong, Xin Feng, and Yana Zhang. Start from video-music  
 530 retrieval: An inter-intra modal loss for cross modal retrieval. *arXiv preprint arXiv:2407.19415*,  
 531 2024b.

532 Zhe Chen, Jiannan Wu, Wenhui Wang, Weijie Su, Guo Chen, Sen Xing, Muyan Zhong, Qing-  
 533 long Zhang, Xizhou Zhu, Lewei Lu, Bin Li, Ping Luo, Tong Lu, Yu Qiao, and Jifeng Dai. In-  
 534 ternVL: Scaling up vision foundation models and aligning for generic visual-linguistic tasks.  
 535 *arXiv preprint arXiv:2312.14238*, 2023.

540 Zhe Chen, Weiyun Wang, Yue Cao, Yangzhou Liu, Zhangwei Gao, Erfei Cui, Jinguo Zhu, Shen-  
 541 glong Ye, Hao Tian, Zhaoyang Liu, et al. Expanding Performance Boundaries of Open-source  
 542 Multimodal Models with Model, Data, and Test-time Scaling. *arXiv preprint arXiv:2412.05271*,  
 543 2024c.

544 Yunfei Chu, Jin Xu, Qian Yang, Haojie Wei, Xipin Wei, Zhifang Guo, Yichong Leng, Yuanjun Lv,  
 545 Jinzheng He, Junyang Lin, Chang Zhou, and Jingren Zhou. Qwen2-Audio Technical Report.  
 546 *arXiv preprint arXiv:2407.10759*, 2024.

548 Jacob Devlin, Ming-Wei Chang, Kenton Lee, and Kristina Toutanova. BERT: Pre-training of deep  
 549 bidirectional Transformers for language understanding. In *Proc. NAACL*, Minneapolis, 2019.

550 Konstantinos Drossos, Samuel Lipping, and Tuomas Virtanen. Clotho: An audio captioning dataset.  
 551 In *Proc. ICASSP*, Barcelona, 2020.

553 Benjamin Elizalde, Soham Deshmukh, Mahmoud Al Ismail, and Huaming Wang. CLAP: Learning  
 554 audio concepts from natural language supervision. In *Proc. ICASSP*, Rhodes Island, 2023.

556 Chaoyou Fu, Yuhang Dai, Yongdong Luo, Lei Li, Shuhuai Ren, Renrui Zhang, Zihan Wang, Chenyu  
 557 Zhou, Yunhang Shen, Mengdan Zhang, et al. Video-MME: The first-ever comprehensive evalua-  
 558 tion benchmark of multi-modal llms in video analysis. In *Proc. CVPR*, Nashville, 2025.

559 Jort F Gemmeke, Daniel PW Ellis, Dylan Freedman, Aren Jansen, Wade Lawrence, R Channing  
 560 Moore, Manoj Plakal, and Marvin Ritter. Audio set: An ontology and human-labeled dataset for  
 561 audio events. In *Proc. ICASSP*, New Orleans, 2017.

562 Yuan Gong, Alexander H. Liu, Hongyin Luo, Leonid Karlinsky, and James Glass. Joint audio and  
 563 speech understanding. In *Proc. ASRU*, Taipei, 2023.

565 Yuan Gong, Hongyin Luo, Alexander H. Liu, Leonid Karlinsky, and James R. Glass. Listen, think,  
 566 and understand. In *Proc. ICLR*, Vienna, 2024.

568 Chenhui Gou, Ziyu Ma, Zicheng Duan, Haoyu He, Feng Chen, Akide Liu, Bohan Zhuang, Jianfei  
 569 Cai, and Hamid Rezatofighi. An empirical study on how video-LLMs answer video questions.  
 570 *arXiv preprint arXiv:2508.15360*, 2025.

571 Tiancheng Gu, Kaicheng Yang, Ziyong Feng, Xingjun Wang, Yanzhao Zhang, Dingkun Long,  
 572 Yingda Chen, Weidong Cai, and Jiankang Deng. Breaking the modality barrier: Universal em-  
 573 bedding learning with multimodal LLMs. In *Proc. ACM MM*, Dublin, 2025.

575 Andrey Guzhov, Federico Raue, Jörn Hees, and Andreas Dengel. AudioCLIP: Extending CLIP to  
 576 image, text and audio. In *Proc. ICASSP*, Singapore, 2022.

577 Mingfei Han, Linjie Yang, Xiaojun Chang, and Heng Wang. Shot2Story20K: A new benchmark for  
 578 comprehensive understanding of multi-shot videos. *arXiv preprint arXiv:2311.17043*, 2023.

580 Dan Hendrycks and Kevin Gimpel. Gaussian error linear units (gelus). *arXiv preprint*  
 581 *arXiv:1606.08415*, 2016.

582 Shawn Hershey, Daniel PW Ellis, Eduardo Fonseca, Aren Jansen, Caroline Liu, R Channing Moore,  
 583 and Manoj Plakal. The benefit of temporally-strong labels in audio event classification. In *Proc.*  
 584 *ICASSP*, Toronto, 2021.

586 Edward J Hu, Yelong Shen, Phillip Wallis, Zeyuan Allen-Zhu, Yuanzhi Li, Shean Wang, Lu Wang,  
 587 Weizhu Chen, et al. LoRA: Low-rank adaptation of large language models. In *Proc. ICLR*, 2022.

588 Chao Jia, Yinfei Yang, Ye Xia, Yi-Ting Chen, Zarana Parekh, Hieu Pham, Quoc Le, Yun-Hsuan  
 589 Sung, Zhen Li, and Tom Duerig. Scaling up visual and vision-language representation learning  
 590 with noisy text supervision. In *Proc. ICML*, 2021.

592 Ting Jiang, Minghui Song, Zihan Zhang, Haizhen Huang, Weiwei Deng, Feng Sun, Qi Zhang,  
 593 Deqing Wang, and Fuzhen Zhuang. E5-V: Universal embeddings with multimodal large language  
 594 models. *arXiv preprint arXiv:2407.12580*, 2024.

594 Ziyuan Jiang, Rui Meng, Xinyi Yang, Semih Yavuz, Yingbo Zhou, and Wenhui Chen. VLM2Vec:  
 595 Training Vision-language Models for Massive Multimodal Embedding Tasks. In *Proc. ICLR*,  
 596 Singapore, 2025.

597

598 Chris Dongjoo Kim, Byeongchang Kim, Hyunmin Lee, and Gunhee Kim. AudioCaps: Generating  
 599 Captions for Audios in The Wild. In *Proc. NAACL-HLT*, Minneapolis, 2019.

600 Ranjay Krishna, Kenji Hata, Frederic Ren, Li Fei-Fei, and Juan Carlos Niebles. Dense-Captioning  
 601 Events in Videos. In *Proc. ICCV*, Venice, 2017.

602

603 Chankyu Lee, Rajarshi Roy, Mengyao Xu, Jonathan Raiman, Mohammad Shoeybi, Bryan Catanzaro,  
 604 and Wei Ping. NV-Embed: Improved techniques for training LLMs as generalist embedding  
 605 models. In *Proc. ICLR*, Singapore, 2025a.

606 Jinyu Lee, Feiyang Chen, Sahil Dua, Daniel Cer, Madhuri Shanbhogue, Iftekhar Naim, Gustavo  
 607 Hernández Ábreo, Zhe Li, Kaifeng Chen, Henrique Schechter Vera, et al. Gemini embedding:  
 608 Generalizable embeddings from gemini. *arXiv preprint arXiv:2503.07891*, 2025b.

609

610 Bo Li, Yuanhan Zhang, Dong Guo, Renrui Zhang, Feng Li, Hao Zhang, Kaichen Zhang, Peiyuan  
 611 Zhang, Yanwei Li, Ziwei Liu, et al. Llava-OneVision: Easy visual task transfer. *Transactions on  
 612 Machine Learning Research*, 2025a.

613 Junnan Li, Dongxu Li, Silvio Savarese, and Steven Hoi. BLIP-2: Bootstrapping language-image  
 614 pre-training with frozen image encoders and large language models. In *Proc. ICML*, Honolulu,  
 615 2023.

616

617 Kunchang Li, Yali Wang, Yinan He, Yizhuo Li, Yi Wang, Yi Liu, Zun Wang, Jilan Xu, Guo Chen,  
 618 Ping Luo, et al. MV-Bench: A comprehensive multi-modal video understanding benchmark. In  
 619 *Proc. CVPR*, Seattle, 2024.

620 Yixuan Li, Changli Tang, Jimin Zhuang, Yudong Yang, Guangzhi Sun, Wei Li, Zejun Ma, and  
 621 Chao Zhang. Improving LLM video understanding with 16 frames per second. In *Proc. ICML*,  
 622 Vancouver, 2025b.

623

624 Sheng-Chieh Lin, Chankyu Lee, Mohammad Shoeybi, Jimmy Lin, Bryan Catanzaro, and Wei Ping.  
 625 MM-Embed: Universal multimodal retrieval with multimodal LLMs. In *Proc. ICLR*, 2025.

626

627 Fuxiao Liu, Yinghan Wang, Tianlu Wang, and Vicente Ordonez. Visual News: Benchmark and  
 628 challenges in news image captioning. In *Proc. EMNLP*, 2021.

629

630 Haotian Liu, Chunyuan Li, Yuheng Li, and Yong Jae Lee. Improved baselines with visual instruction  
 631 tuning. In *Proc. CVPR*, Seattle, 2024a.

631

632 Haotian Liu, Chunyuan Li, Qingyang Wu, and Yong Jae Lee. Visual instruction tuning. In *Proc.  
 633 NeurIPS*, Vancouver, 2024b.

634

635 Yikun Liu, Yajie Zhang, Jiayin Cai, Xiaolong Jiang, Yao Hu, Jiangchao Yao, Yanfeng Wang, and  
 636 Weidi Xie. LamRA: Large multimodal model as your advanced retrieval assistant. In *Proc. CVPR*,  
 637 Nashville, 2025a.

637

638 Zhijian Liu, Ligeng Zhu, Baifeng Shi, Zhuoyang Zhang, Yuming Lou, Shang Yang, Haocheng Xi,  
 639 Shiyi Cao, Yuxian Gu, Dacheng Li, et al. NVILA: Efficient frontier visual language models. In  
 640 *Proc. CVPR*, Nashville, 2025b.

641

642 Yawei Ma, Guohai Xu, Xiaoshuai Sun, Ming Yan, Ji Zhang, and Rongrong Ji. X-CLIP: End-to-end  
 643 multi-grained contrastive learning for video-text retrieval. In *Proc. ACM MM*, Lisbon, 2022.

644

645 Ziyang Ma, Yinghao Ma, Yanqiao Zhu, Chen Yang, Yi-Wen Chao, Ruiyang Xu, Wenxi Chen,  
 646 Yuanzhe Chen, Zhuo Chen, Jian Cong, et al. MMAR: A challenging benchmark for deep reasoning  
 647 in speech, audio, music, and their mix. *arXiv preprint arXiv:2505.13032*, 2025.

648

649 Karttikeya Mangalam, Raiymbek Akshulakov, and Jitendra Malik. EgoSchema: A diagnostic bench-  
 650 mark for very long-form video language understanding. *Proc. NIPS*, 2023.

648 Daniel McKee, Justin Salamon, Josef Sivic, and Bryan Russell. Language-guided music recom-  
 649 mendation for video via prompt analogies. In *Proc. CVPR*, Vancouver, 2023.  
 650

651 Xinhao Mei, Chutong Meng, Haohe Liu, Qiuqiang Kong, Tom Ko, Chengqi Zhao, Mark D Plumb-  
 652 ley, Yuexian Zou, and Wenwu Wang. WavCaps: A ChatGPT-assisted weakly-labelled audio  
 653 captioning dataset for audio-language multimodal research. *IEEE/ACM Transactions on Audio,*  
*654 Speech, and Language Processing*, 32:3339–3354, 2024.

655 Rui Meng, Ziyan Jiang, Ye Liu, Mingyi Su, Xinyi Yang, Yuepeng Fu, Can Qin, Zeyuan Chen,  
 656 Ran Xu, Caiming Xiong, et al. VLM2Vec-V2: Advancing Multimodal Embedding for Videos,  
 657 Images, and Visual Documents. *arXiv preprint arXiv:2507.04590*, 2025.

658 Antoine Miech, Jean-Baptiste Alayrac, Lucas Smaira, Ivan Laptev, Josef Sivic, and Andrew Zisser-  
 659 man. End-to-end learning of visual representations from uncurated instructional videos. In *Proc.*  
*660 CVPR*, Seattle, 2020.

661 Niklas Muennighoff, Nouamane Tazi, Loïc Magne, and Nils Reimers. MTEB: Massive text embed-  
 662 ding benchmark. In *Proc. EACL*, Dubrovnik, 2022.

663 Matthew E Peters, Mark Neumann, Mohit Iyyer, Matt Gardner, Christopher Clark, Kenton Lee,  
 664 and Luke Zettlemoyer. Deep contextualized word representations. In *Proc. NAACL-HLT*, New  
 665 Orleans, 2018.

666 Alec Radford, Jong Wook Kim, Chris Hallacy, Aditya Ramesh, Gabriel Goh, Sandhini Agarwal,  
 667 Girish Sastry, Amanda Askell, Pamela Mishkin, Jack Clark, et al. Learning transferable visual  
 668 models from natural language supervision. In *Proc. ICML*, 2021.

669 Alec Radford, Jong Wook Kim, Tao Xu, Greg Brockman, Christine McLeavey, and Ilya Sutskever.  
 670 Robust speech recognition via large-scale weak supervision. In *Proc. ICML*, Honolulu, 2023.

671 S Sakshi, Utkarsh Tyagi, Sonal Kumar, Ashish Seth, Ramaneswaran Selvakumar, Oriol Nieto, Ra-  
 672 mani Duraiswami, Sreyan Ghosh, and Dinesh Manocha. MMAU: A massive multi-task audio  
 673 understanding and reasoning benchmark. In *Proc. ICLR*, Singapore, 2025.

674 Kun Su, Xiulong Liu, and Eli Shlizerman. From vision to audio and beyond: A unified model for  
 675 audio-visual representation and generation. In *Proc. ICML*, Vienna, 2024.

676 Changli Tang, Wenyi Yu, Guangzhi Sun, Xianzhao Chen, Tian Tan, Wei Li, Lu Lu, Zejun MA, and  
 677 Chao Zhang. SALMONN: Towards generic hearing abilities for large language models. In *Proc.*  
*678 ICLR*, Vienna, 2024.

679 Changli Tang, Yixuan Li, Yudong Yang, Jimin Zhuang, Guangzhi Sun, Wei Li, Zejun Ma, and Chao  
 680 Zhang. video-SALMONN 2: Captioning-enhanced audio-visual large language models. *arXiv*  
 681 *preprint arXiv:2506.15220*, 2025.

682 Liang Wang, Nan Yang, Xiaolong Huang, Linjun Yang, Rangan Majumder, and Furu Wei. Improv-  
 683 ing text embeddings with large language models. In *Proc. ACL*, Bangkok, 2024.

684 Xin Wang, Jiawei Wu, Junkun Chen, Lei Li, Yuan-Fang Wang, and William Yang Wang. VATEX:  
 685 A large-scale, high-quality multilingual dataset for video-and-language research. In *Proc. ICCV*,  
 686 Seoul, 2019.

687 Junbin Xiao, Xindi Shang, Angela Yao, and Tat-Seng Chua. NExT-QA: Next phase of question-  
 688 answering to explaining temporal actions. In *Proc. CVPR*, 2021.

689 Hu Xu, Gargi Ghosh, Po-Yao Huang, Dmytro Okhonko, Armen Aghajanyan, Florian Metze, Luke  
 690 Zettlemoyer, and Christoph Feichtenhofer. VideoCLIP: Contrastive pre-training for zero-shot  
 691 video-text understanding. In *Proc. EMNLP*, Punta Cana, 2021.

692 Jin Xu, Zhifang Guo, Jinzheng He, Hangrui Hu, Ting He, Shuai Bai, Keqin Chen, Jialin Wang, Yang  
 693 Fan, Kai Dang, et al. Qwen2.5-Omni technical report. *arXiv preprint arXiv:2503.20215*, 2025.

694 Jun Xu, Tao Mei, Ting Yao, and Yong Rui. MSR-VTT: A large video description dataset for bridging  
 695 video and language. In *Proc. CVPR*, Las Vegas, 2016.

702 Hao Yu, Zhuokai Zhao, Shen Yan, Lukasz Korycki, Jianyu Wang, Baosheng He, Jiayi Liu, Lizhu  
 703 Zhang, Xiangjun Fan, and Hanchao Yu. CAFE: Unifying representation and generation with  
 704 contrastive-autoregressive finetuning. *arXiv preprint arXiv:2503.19900*, 2025a.

705

706 Peng Yu, En Xu, Bin Chen, Haibiao Chen, and Yinfei Xu. QZhou-Embedding technical report.  
 707 *arXiv preprint arXiv:2508.21632*, 2025b.

708 Zhou Yu, Dejing Xu, Jun Yu, Ting Yu, Zhou Zhao, Yueling Zhuang, and Dacheng Tao. ActivityNet-  
 709 QA: A dataset for understanding complex web videos via question answering. In *Proc. AAAI*,  
 710 Hawaii, 2019.

711

712 Xiaohua Zhai, Basil Mustafa, Alexander Kolesnikov, and Lucas Beyer. Sigmoid loss for language  
 713 image pre-training. In *Proc. ICCV*, Paris, 2023.

714 Boqiang Zhang, Kehan Li, Zesen Cheng, Zhiqiang Hu, Yuqian Yuan, Guanzheng Chen, Sicong  
 715 Leng, Yuming Jiang, Hang Zhang, Xin Li, et al. VideoLLaMA 3: Frontier Multimodal Foundation  
 716 Models for Image and Video Understanding. *arXiv preprint arXiv:2501.13106*, 2025a.

717

718 Xin Zhang, Yanzhao Zhang, Wen Xie, Mingxin Li, Ziqi Dai, Dingkun Long, Pengjun Xie, Meishan  
 719 Zhang, Wenjie Li, and Min Zhang. GME: Improving universal multimodal retrieval by multi-  
 720 modal llms. *arXiv preprint arXiv:2412.16855*, 2024.

721 Yanzhao Zhang, Mingxin Li, Dingkun Long, Xin Zhang, Huan Lin, Baosong Yang, Pengjun Xie,  
 722 An Yang, Dayiheng Liu, Junyang Lin, et al. Qwen3 embedding: Advancing text embedding and  
 723 reranking through foundation models. *arXiv preprint arXiv:2506.05176*, 2025b.

724

725 Yuanhan Zhang, Jinming Wu, Wei Li, Bo Li, Zejun Ma, Ziwei Liu, and Chunyuan Li. Video  
 726 instruction tuning with synthetic data. *Transactions on Machine Learning Research*, 2025c.

727 Luwei Zhou, Chenliang Xu, and Jason Corso. Towards automatic learning of procedures from web  
 728 instructional videos. In *Proc. AAAI*, New Orleans, 2018.

729

730 Jinguo Zhu, Weiyun Wang, Zhe Chen, Zhaoyang Liu, Shenglong Ye, Lixin Gu, Hao Tian, Yuchen  
 731 Duan, Weijie Su, Jie Shao, et al. InternVL3: Exploring advanced training and test-time recipes  
 732 for open-source multimodal models. *arXiv preprint arXiv:2504.10479*, 2025.

733

## 734 A THE USE OF LARGE LANGUAGE MODELS

735 We used Gemini-2.5-Pro to help us check for grammar errors and polish the fluency of our sentences.

## 736 B INFERENCE PROCEDURE FOR EVALUATION TASKS

737 The evaluation tasks can also be divided into two categories: retrieval tasks and QA tasks. Tasks  
 738 that use a single, unified general prompt to extract embeddings for all test samples are regarded as  
 739 retrieval tasks. This includes the classification, retrieval, and moment retrieval subsets of MMEB-v2-  
 740 Video. Conversely, tasks that use separate and specific questions as prompts to extract embeddings  
 741 are considered QA tasks.

742 For all retrieval tasks, we generate an embedding for each sample in the test set based on its input  
 743 video/audio, using the fixed text prompt, "Please describe the video/audio." If the task involves re-  
 744 trieving text, the corresponding ground-truth text captions for each sample are also used to generate  
 745 text embeddings. The entire test set then forms the candidate pool for the retrieval task. The candi-  
 746 date with the highest similarity score to the query embedding is selected as the model's prediction.

747 For QA tasks, all QA evaluations for the embedding LLMs are performed using an embedding-based  
 748 methodology. To be specific, the inference procedure is as follows:

749

- 750 1. The model first generates a single embedding that is conditioned on both the source modality  
 751 (video/audio) and the provided question text.
- 752 2. Separately, the model generates an embedding for the text of each answer option.

756 3. The similarity between the question-conditioned video/audio embedding and each of the option  
 757 text embeddings is then calculated.  
 758 4. The option with the highest similarity score is selected as the model’s predicted answer.  
 759

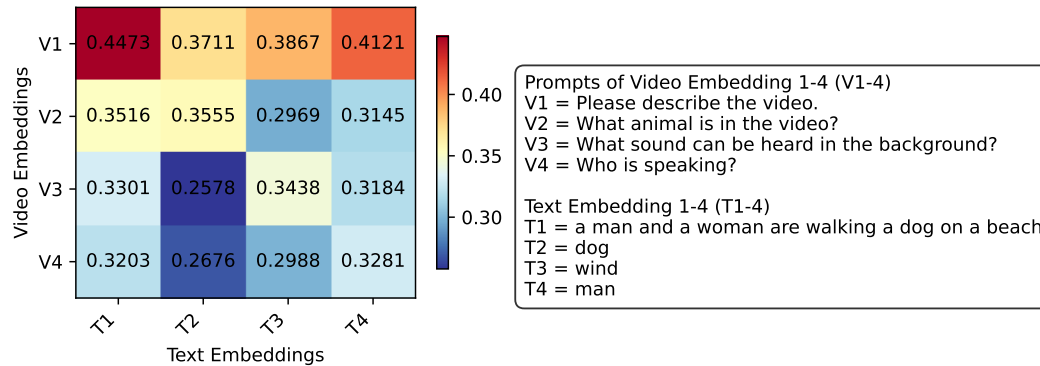
760 **C MORE EVALUATION RESULTS OF WAVE**

763 In the retrieval task of MMEB-v2-Video, only one direction, text-to-video retrieval, was evaluated.  
 764 Similarly, for the audio retrieval and audio-visual retrieval tasks presented in Table 4, only a single  
 765 direction was assessed, i.e, text-to-audio and video-to-audio retrieval, respectively. This focus  
 766 was chosen because these directions more closely align with practical, real-world application sce-  
 767 narios like multimodal search and recommendation. However, it is undeniable that performance in  
 768 the reverse direction is also important. In Table 8, we provide supplementary results for video re-  
 769 trieval (V-RET), audio retrieval (A-RET), and audio-visual retrieval (AV-RET) in the other direction.  
 770 WAVE can also achieve competitive results in the other direction.

771  
 772 Table 8: Results of video-to-text, audio-to-text and audio-to-video retrieval. Corresponding refer-  
 773 ence models and their scores are also provided.

Method	V-RET			A-RET		AV-RET	
	MSR-VTT	VATEX	YouCook2	Clotho	VGGSound		
Reference Model	GME 7B (Zhang et al., 2024)			(Mei et al., 2024)	encoder-only retrieval model (ours)		
Reference Value	32.2	33.0	10.0	<b>27.1</b>	8.2		
WAVE 7B	<b>55.1</b>	<b>55.4</b>	<b>29.8</b>	24.5		<b>25.8</b>	

780  
 781 **D CASE STUDY OF PROMPT-AWARE EMBEDDINGS**  
 782



797 Figure 2: A heatmap visualizing the cosine similarity between video embeddings (V1-V4) and text  
 798 embeddings (T1-T4). All four video embeddings are generated from the **same video** but conditioned  
 799 on different textual prompts. The text embeddings represent various concepts present in the video.

800 To provide a more intuitive and qualitative demonstration of WAVE’s prompt-aware embedding ca-  
 801 pability, we conduct a case study on a single video. We select a video from the MSR-VTT test set,  
 802 which shows a man and a woman walking a dog on a beach, with wind blowing in the background.  
 803 We then generated four distinct embeddings (V1-V4) for this single video conditioned on different  
 804 prompts, ranging from a general description request to specific questions about visual animals, back-  
 805 ground sounds, or speakers. Concurrently, we generated four text embeddings (T1-T4) representing  
 806 a general description and the specific concepts of “dog”, “wind”, and “man”.

808 The cosine similarities between these video and text embeddings are visualised in the heatmap in  
 809 Figure 2. The general prompt V1 (“Please describe the video.”) yields an embedding that has the  
 highest similarity (0.4473) with the general text description T1. In addition, video embeddings

810 conditioned on prompts about specific aspects of the video (V2, V3, V4) also show high similarity  
 811 to T1, indicating that these prompt-aware embeddings still retain the overall semantic context of the  
 812 video. In addition, video embeddings generated from specific prompts are clearly biased towards  
 813 the textual representation of that specific feature. For instance, the embedding V2, generated by the  
 814 prompt "What animal is in the video?", has a slightly higher similarity than T1 and a significantly  
 815 higher similarity with T2 ("dog") than with T3 ("wind") or T4 ("man"). Similarly, the audio-focused  
 816 V3 aligns best with "wind" (T3), and the speaker-focused V4 matches most closely with "man"  
 817 (T4). This clearly demonstrates that WAVE can dynamically shift the semantic focus of its output  
 818 embedding to produce a representation that is precisely tailored to the user's query.

## E ANALYSIS OF DUAL SPEECH & AUDIO ENCODERS

820 Speech and general audio events are both crucial elements within an audio signal. Our base model,  
 821 Qwen2.5-Omni, possesses some capability to process general audio, but its encoder for audio pro-  
 822 cessing is derived from Whisper (Radford et al., 2023), a model optimised for automatic speech  
 823 recognition. This speech encoder, which is primarily specialised for modelling speech, has an insuf-  
 824 ficient understanding of non-speech audio events. To address this limitation, we augment the existing  
 825 speech encoder with a dedicated audio encoder, BEATs (Chen et al., 2022b), which is designed for  
 826 comprehensive audio event understanding.

827 To validate the effectiveness of this dual-encoder approach, we compared its performance on video  
 828 retrieval, audio retrieval, and audio-visual retrieval, respectively, with that of using only the original  
 829 speech encoder. For video retrieval, we test the models on MSR-VTT, VATEX, and YouCook2,  
 830 whose videos are paired with audio. The results are presented in Table 9. The dual-encoder con-  
 831 figuration consistently outperforms the single speech encoder on both the audio retrieval and audio-  
 832 visual retrieval, and achieves comparable or better performance on video retrieval benchmarks. This  
 833 indicates that the speech and audio encoders can complement each other to further enhance the  
 834 model's ability to interpret both speech and environmental sounds.

835 Table 9: Results of using dual speech and audio encoders and using a speech encoder only. Video  
 836 retrieval (V-RET), audio retrieval (A-RET), and audio-visual retrieval (AV-RET) are evaluated here.

Method	V-RET			A-RET			AV-RET	
	MSR-VTT	VATEX	YouCook2	AudioCaps	Clotho	VGGSound	MusicCaps	
Single speech encoder	<b>58.6</b>	56.6	34.3	39.6	22.4	23.3	18.3	
Dual speech & audio encoders	58.5	<b>58.4</b>	<b>36.8</b>	<b>42.5</b>	<b>24.0</b>	<b>24.9</b>	<b>20.1</b>	

## F THE EFFECT OF IMAGE TRAINING

840 WAVE is primarily trained on video data and achieves strong performance on video retrieval-related  
 841 tasks. However, this success is not due to a narrow specialization in video. In fact, WAVE is  
 842 not specialized only for video retrieval, and image data actually helps. In a preliminary study, we  
 843 compared the results of training solely on video data against training on a mixture of video data and  
 844 a nearly equal amount of image data from the MMEB-v1 training set. This experiment utilized the  
 845 same pure-visual video retrieval setup as described in Section 5.4. Table 10 presents the results of  
 846 this comparison.

847 Table 10: Comparison of results for training with and without image data. We evaluate text-to-  
 848 image retrieval (Liu et al., 2021) on the VisualNews dataset and text-to-video retrieval on MMEB-  
 849 v2-Video.

Training Data	Image RET		MMEB-v2-Video RET				
	VisualNews	Average	MSR-VTT	VATEX	MSVD	DiDeMo	YouCook2
Video Data	54.9	49.6	52.1	46.2	<b>69.7</b>	53.0	27.2
Video Data + Image Data (MMEB-v1)	<b>74.8</b>	<b>50.2</b>	<b>52.4</b>	<b>46.2</b>	69.0	<b>55.8</b>	<b>27.8</b>

864 As the results show, including image data substantially improves image retrieval and provides a  
865 slight gain in video retrieval. This shows that WAVE’s strong performance is not due to avoiding  
866 image tasks or specializing exclusively in video.  
867  
868  
869  
870  
871  
872  
873  
874  
875  
876  
877  
878  
879  
880  
881  
882  
883  
884  
885  
886  
887  
888  
889  
890  
891  
892  
893  
894  
895  
896  
897  
898  
899  
900  
901  
902  
903  
904  
905  
906  
907  
908  
909  
910  
911  
912  
913  
914  
915  
916  
917